

RESEARCH

Open Access



^{18}F -FDG PET/CT metabolic parameter changes to assess vascular inflammatory response in patients with diffuse large B-cell lymphoma

Wenli Xie^{1†}, Lixiu Cao^{2,3†}, Jing Yu⁴, Aijuan Tian⁴, Jin Wang^{5,7*} and Runlong Lin^{4,6*}

Abstract

Objective To study the changes in positron emission tomography with 2-deoxy-2-[fluorine-18]fluoro-D-glucose integrated with computed tomography (^{18}F -FDG PET/CT) aortic target-to-background ratio (TBR) and aortic calcification scores before and after 6 cycles of chemotherapy with the rituximab, cyclophosphamide, doxorubicin, vincristine, and prednisone (R-CHOP) regimen in patients with diffuse large B-cell lymphoma (DLBCL).

Patients and methods We selected 161 patients with DLBCL who received 6 cycles of R-CHOP standard chemotherapy and underwent baseline and 6-cycle efficacy evaluations using ^{18}F -FDG PET/CT examinations at the Second Hospital of Dalian Medical University from July 2017 to June 2023. Additionally, 125 patients who underwent ^{18}F -FDG PET/CT for physical examination during the same period, without active malignancy or systemic inflammatory disease, were chosen as the control group. We measured metabolic tumor volume (MTV) and total lesion glycolysis (TLG) of systemic lymphoma lesions in tumor patients. Aortic wall FDG uptake was semi quantitatively analyzed as TBR (target-to-blood pool ratio) in five different vascular regions using oncological ^{18}F -FDG PET/CT. The aortic TBR difference (ΔTBR) was the difference between the post- and pre-chemotherapy TBR values. The degree of arterial segmental wall calcification was assessed using the CT semiquantitative method.

Results Comparison of the pre-treatment group of DLBCL with the control group showed that aortic TBR (1.28 ± 0.17 vs. 1.22 ± 0.18 , $P < 0.05$) were higher in the former group. Additionally, comparing different stage groups of patients with DLBCL revealed that aortic TBR (1.30 ± 0.18 vs. 1.22 ± 0.15 , $P < 0.05$) were higher in the Stage III/IV group compared to the Stage I/II group. Aortic TBR was positively correlated with TLG ($P = 0.016$, $R = 0.19$) and MTV ($P = 0.032$, $R = 0.17$). Analysis of changes in aortic ^{18}F -FDG uptake in patients with DLBCL after 6 cycles of treatment revealed that aortic TBR levels were significantly higher post-treatment compared to pre-treatment ($P < 0.05$). The aortic ΔTBR value was significantly higher in the progression group than in the complete remission group ($P < 0.05$).

[†]Wenli Xie and Lixiu Cao contributed equally to this work.

*Correspondence:

Jin Wang

919119655@qq.com

Runlong Lin

longjunji1129@126.com

Full list of author information is available at the end of the article



Conclusion Aortic wall ^{18}F -FDG uptake is related to disease severity and prognosis, indicating a possible vascular effect of lymphoma and its therapeutic interventions. This work highlights an additional potential role of PET/CT in imaging oncology for evaluating disease severity and its consequences on the vasculature.

Keywords Diffuse large B-cell lymphoma, Tumor-associated vascular toxicity, Vascular inflammation, ^{18}F -FDG PET/CT

Introduction

Malignant tumors and cardiovascular disease are the two leading causes of death in humans [1]. Oncology patients may experience vascular toxicity during and after chemotherapy [2]. The diversity of vascular toxicity from oncology treatments, including altered vascular reactivity, vascular thrombosis, atherosclerosis, and vasculitis, leading to vascular lumen obstruction and decreased blood flow, requires joint attention from cardiovascular physicians and oncologists [3]. The pathophysiologic mechanisms are not fully understood, but inflammatory cell aggregation and cytokine production after drug treatment, leading to an inflammatory response in the arterial wall, are important causes [4]. A localized vessel wall inflammatory response plays a crucial role in atherogenesis, which can lead the progression of atherosclerosis and cause cardiovascular and cerebrovascular diseases [5]. Therefore, early identification of vascular wall inflammatory reactions is important for predicting patients at high risk for future cardiovascular events.

2-deoxy-2-[fluorine-18]fluoro-D-glucose (^{18}F -FDG) accumulation in the vessel wall increases due to the glycolytic process of the inflammatory response, and positron emission tomography with 2-deoxy-2-[fluorine-18]fluoro-D-glucose integrated with computed tomography (^{18}F -FDG PET/CT) can be used to assess vascular inflammation [6, 7]. ^{18}F -FDG PET/CT imaging focuses on quantifying vascular inflammation in different segments of the arterial system with higher sensitivity and can detect vascular ^{18}F -FDG uptake in parallel with tumor imaging to assess vascular inflammation.

Arterial calcification has become a hallmark of atherosclerosis and is easily recognized on CT imaging [8]. Shen et al. [9] predicted cancer treatment-related cardiac dysfunction and major adverse cardiovascular events in patients with diffuse large B-cell lymphoma (DLBCL) receiving anthracycline-based chemotherapy by evaluating pre-treatment coronary artery calcification (CAC) scores. They found that CAC scores obtained by pre-treatment CT were useful in identifying patients at high risk of developing cardiac events after treatment and in guiding clinicians to relevant cardiovascular protection strategies for high-risk patients. Therefore, ^{18}F -FDG PET/CT can be used to assess the level of vascular wall metabolism, calcification, and changes during the diagnosis and follow-up of tumor patients, and to identify patients at high risk of vascular disease at an early stage [10]. In this study, we observed the changes in the level of

aortic inflammation and calcification during 6 cycles of treatment with the rituximab, cyclophosphamide, doxorubicin, vincristine, and prednisone (R-CHOP) standard chemotherapy regimen in patients with diffuse large B-cell lymphoma using ^{18}F -FDG PET/CT.

Methods

Patients

161 patients with DLBCL who received 6 cycles of the R-CHOP standard chemotherapy regimen at the Second Hospital of Dalian Medical University from July 2017 to June 2023 and underwent baseline and post-6-cycle evaluation with two ^{18}F -FDG PET/CT examinations, with complete case data, were selected. The standard R-CHOP chemotherapy regimen included cyclophosphamide 750 mg/m^2 on day 1, adriamycin 50 mg/m^2 on day 1, vincristine 1.4 mg/m^2 on day 1, prednisone 100 mg on days 1–5, and rituximab 375 mg/m^2 on day 1. Inclusion criteria: (1) Patients with pathologically confirmed diffuse large B-cell lymphoma, who underwent ^{18}F -FDG PET/CT imaging before chemotherapeutic treatment and within 3 weeks after 6 cycles of treatment; (2) Detailed inquiry of cardiac history after admission, white blood cell, neutrophil, lymphocyte, lactate dehydrogenase, albumin, blood sedimentation, CRP and other tests. Exclusion criteria: (1) Poor quality of PET/CT images; (2) Incomplete case data of the patients to be collected; (3) Previous history of tumor, who have received radiotherapy or chemotherapy; (4) Diabetic patients with poor glycemic control; (5) Those with severe liver and kidney dysfunction; (6) Those with focal involvement of the heart (e.g., tumor, tuberculosis, etc.); (7) Recent cardiovascular events (<6 months); (8) Those with aortitis, active infections or systemic autoimmune diseases, venous thromboembolism and application of anti-inflammatory drug therapy, and infection with COVID-19; (9) Patients whose arterial ^{18}F -FDG uptake could not be quantified due to significant interference from adjacent lymphoma. The enrolled DLBCL patients are shown in the flow diagram, show in Fig. 1. Additionally, 125 patients who underwent ^{18}F -FDG PET/CT at the Second Hospital of Dalian Medical University during the same period for mildly elevated tumor markers, fever of unknown origin and physical examination, without active malignant tumors or systemic inflammatory diseases, were selected as the control group. The study conforms to the ethical guidelines in accordance with the Helsinki Declaration and was approved by the Second Hospital of Dalian Medical University review

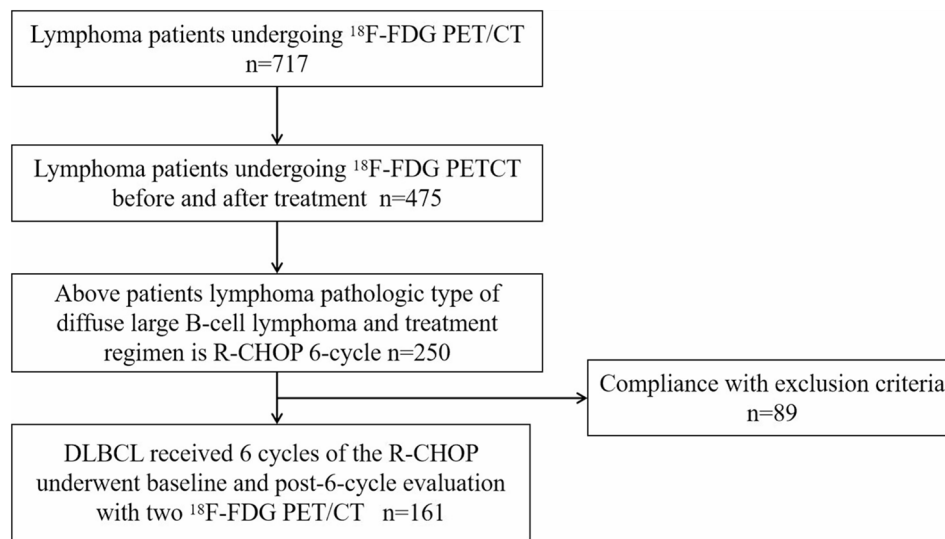


Fig. 1 The flow diagram of eligible DLBCL patients

board and ethical committee (No.2019-049). Written informed consent was obtained from every patient.

Collection of clinical data

The outpatient and inpatient medical records and PET/CT examination transcripts were reviewed to collect general clinical data of the patients, including age, gender, hypertension, diabetes, history of heart disease, history of radiotherapy and/or chemotherapy, purpose of PET/CT imaging, blood tests (including white blood cell, neutrophil, lymphocyte, lactate dehydrogenase, β 2-microglobulin, blood sedimentation, C-reactive protein, etc.), and the clinical stage of lymphoma.

^{18}F -FDG PET/CT examination

We used the Philips Ingenuity TF PET/CT scanner for the assessments. The ^{18}F -FDG was produced and synthesized using the Sumitomo HM-10 cyclotron accelerator and the chemical synthesis module from PET CO., LTD. (Beijing), ensuring a radiochemical purity exceeding 95%. Patients fasted for at least 12 h before the procedure. After administering ^{18}F -FDG at a dosage of 3.7–5.55 MBq/kg, patients rested in a dimly lit room for 60 min before undergoing PET/CT scans post-bladder voiding. The scan ranged from the skull base to the foot. Initially, CT scans were performed with parameters set at a voltage of 120 kV, current of 90 mA, rotation speed of 0.75 s/rotation, and a matrix of 512×512 . Subsequently, PET imaging followed with conditions set at a matrix of 144×144 and 1-minute acquisition for each bed position, totaling 8–10 bed positions. After attenuation correction and OSEM reconstruction, PET images were co-registered with CT images on the image processing workstation.

Image analysis

All PET/CT images were retrospectively analyzed by two experienced nuclear medicine physicians with more than 10 years of experience blinded to the clinical data. Any different opinions between the two physicians were discussed to reach an agreement. The region of interest (ROI) of tumor foci was outlined layer by layer on tomographic PET/CT fusion images. The metabolic tumor volume (MTV) and total lesion glycolysis (TLG) were measured automatically using the SUV-based automated contouring program with the relative thresholding method, which uses 41% of the tumor foci SUVmax as the threshold value. MedEx software, provided by Beijing MedEx Technology Co., was used for these measurements. The sum of TLG values of systemic tumor lesions was calculated as $\text{TLG} = \sum(\text{SUVmean} \times \text{MTV})$ [11]. ROIs in the aortic wall were manually drawn along the entire aortic interval in 5 mm consecutive axial sections. Care was taken to ensure activity from adjacent tissue or adjacent lymphoma was not included in the aortic analysis. The metabolic activity of these ROIs was measured using the maximum SUV (SUVmax). Six zones of interest, each 3 mm in diameter, were drawn within the superior vena cava, and the mean venous SUV (SUVmean) was calculated. The arterial target-to-background ratio (TBR) was determined by dividing the mean aortic SUVmax by the superior vena cava SUVmean. The aortic TBR was calculated by averaging the TBRs of the ascending aorta, aortic arch, descending aorta, suprarenal abdominal aorta, and infrarenal abdominal aorta, i.e., $\text{aortic TBR} = (\text{ascending aorta TBR} + \text{aortic arch TBR} + \text{descending aorta TBR} + \text{suprarenal abdominal aorta TBR} + \text{infrarenal abdominal aorta TBR}) \div 5$ [12–15]. The change in aortic TBR, aortic ΔTBR , was defined as the aortic TBR after 6 cycles of treatment minus the aortic TBR at initial

diagnosis, i.e., Δ aortic TBR = aortic TBR_{6 cycles} - aortic TBR_{pre-treatment}. The degree of arterial segmental wall calcification was assessed using the ¹⁸F-FDG PET/CT semi-quantitative method. The score was based on the percentage of calcified plaque in the truncated circumference of the same vessel. The scoring system was as follows: no calcified plaque scored 0, calcified plaque <10% scored 1, calcified plaque 10–25% scored 2, calcified plaque 25–50% scored 3, and calcified plaque >50% scored 4. Calcified plaques in the ascending aorta, aortic arch, descending aorta, suprarenal abdominal aorta, and infrarenal abdominal aorta were scored, with a total possible score ranging from 0 to 20 [16, 17].

Statistical analysis

SPSS Statistics 26.0 was used for analysis. Continuous variables were tested for normality using the Kolmogorov-Smirnov test. Normally distributed measures were expressed as mean \pm standard deviation ($X \pm S$), non-normally distributed measures were expressed as median (P25, P75), and categorical variables were expressed as number and percentage (%). Differences between two independent samples were analyzed using the t-test or Mann-Whitney U-test, and the ggplot2 package was used for box plot and violin plot visualization. One-way ANOVA analysis or Kruskal-Wallis H test was used to analyze the difference between three and more independent samples. Bonferroni correction was applied to

P-values to adjust for multiple testing. The Bonferroni correction for P-values sets the significance cut-off at P/n , where P is 0.05 and n is the number of tests. The χ^2 test was used to compare rates between two independent samples. The Spearman/Pearson test was used to analyze the correlation between two independent samples, and the ggplot2 package was used to visualize the heatmap for correlation analysis. A p-value <0.05 was considered statistically significant.

Results

Comparison of clinical characteristics and ¹⁸F-FDG PET/CT parameters between pre-treatment and control groups of diffuse large B-cell lymphoma

Comparing the clinical data between the pre-treatment group of diffuse large B-cell lymphoma and the control group, it was found that the age of patients with diffuse large B-cell lymphoma was significantly higher than that of the control group ($P < 0.05$). The other factors, including gender, body surface area, hypertension, diabetes mellitus, coronary artery disease, and atrial fibrillation history, did not show significant differences compared to the control group ($P > 0.05$). Among the patients with diffuse large B-cell lymphoma, the Ann Arbor stages were as follows: 6 in stage I, 33 in stage II, 30 in stage III, and 92 in stage IV. Additionally, 133 patients were in group A, and 28 patients were in group B. Comparing blood biomarker levels between the pre-treatment group and the control group, it was observed that the white blood cell (WBC) count in patients with diffuse large B-cell lymphoma was lower than in the control group, while albumin levels were higher; however, these differences were not statistically significant ($P > 0.05$). The neutrophil-to-lymphocyte ratio (N/L) and lactate dehydrogenase (LDH) levels in patients with diffuse large B-cell lymphoma at initial diagnosis were significantly higher than those in the control group ($P < 0.05$). See Table 1.

Patients with diffuse large B-cell lymphoma underwent baseline ¹⁸F-FDG PET/CT evaluation before treatment. The TLG value was 846.67 (246.65, 3113.25) g, and the MTV value was 93.31 (31.62, 245.88) cm³. Before treatment, the aortic calcification score in these patients was significantly higher than in the control group, and the difference was statistically significant. Comparing aortic ¹⁸F-FDG uptake between the two groups, we found that the aortic TBR and TBR values of each segment of the aorta in patients with diffuse large B-cell lymphoma were significantly higher than in the control group before treatment ($P < 0.05$). See Table 2.

Table 1 Comparison of clinical data between pre-treatment group and control group for diffuse large B-cell lymphoma

	Diffuse large B-cell lymphoma pre-treatment group (N=161)	Control group (N=125)	P value
Age(years)	59.75 \pm 11.29	55.33 \pm 13.41	0.003
Male(n, %)	72(44.72)	64(51.20)	0.276
BSA(m ²)	1.76 \pm 0.18	1.76 \pm 0.22	0.985
Hypertension(n, %)	36(22.36)	22(17.60)	0.321
Diabetes (n, %)	23(14.29)	18(14.40)	0.978
Coronary artery disease (n, %)	6(3.73)	9(7.20)	0.191
Atrial fibrillation (n, %)	4(2.48)	2(1.6)	0.605
Ann Arbor stage			
I/II	6/33	—	
III/IV	30/92	—	
A/B	133/28	—	
WBC($\times 10^9/L$)	6.25 \pm 2.85	6.79 \pm 2.11	0.078
N/L	3.65 \pm 2.66	2.94 \pm 1.60	0.01
ESR(mm/h)	15.00(9.00, 25.00)	—	
LDH(μ g/mL)	306.27 \pm 222.17	187.38 \pm 39.81	0.001
Alb(g/L)	39.79 \pm 5.70	38.56 \pm 5.49	0.069
β 2-MG(mg/L)	3.08 \pm 1.18	—	

Abbreviations: BSA, body surface area; WBC: white blood cell; N/L: neutrophil-to-lymphocyte ratio; ESR: erythrocyte sedimentation rate; LDH: lactate dehydrogenase; ALB: albumin; β 2-MG: β 2 microglobulin

Table 2 Comparison of ¹⁸F-FDG PET/CT parameters between pre-treatment group and control group for diffuse large B-cell lymphoma

	Diffuse large B-cell lymphoma pre-treatment group(N= 161)	Control group(N= 125)	P value
Aortic Calcification Score _{pre-treatment}	5.00(3.00, 7.00)	2.00(0.50, 4.00)	0.001
TLG _{pre-treatment} g	846.67(246.65, 3113.25)	—	
MTV _{pre-treatment} cm ³	93.31(31.62, 245.88)	—	
Ascending aorta TBR _{pre-treatment}	1.33±0.18	1.28±0.17	0.017
Aortic arch TBR _{pre-treatment}	1.27±0.18	1.21±0.20	0.006
Descending aorta TBR _{pre-treatment}	1.26±0.20	1.21±0.20	0.034
Suprarenal abdominal aorta TBR _{pre-treatment}	1.28±0.18	1.21±0.19	0.001
Infrarenal abdominal aorta TBR _{pre-treatment}	1.26±0.18	1.19±0.18	0.002
Aortic TBR _{pre-treatment}	1.28±0.17	1.22±0.18	0.004

Abbreviations: MTV: metabolic tumor volume; TLG: total lesion glycolysis

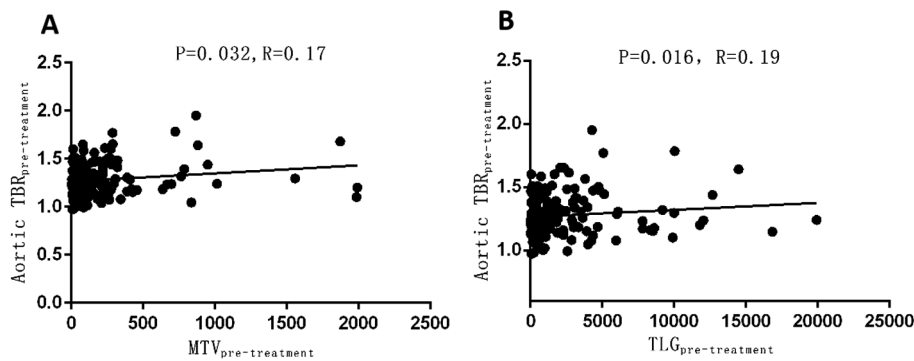


Fig. 2 Correlation between aortic ¹⁸F-FDG uptake and tumor metabolic load in pre-treatment patients with diffuse large B-cell lymphoma

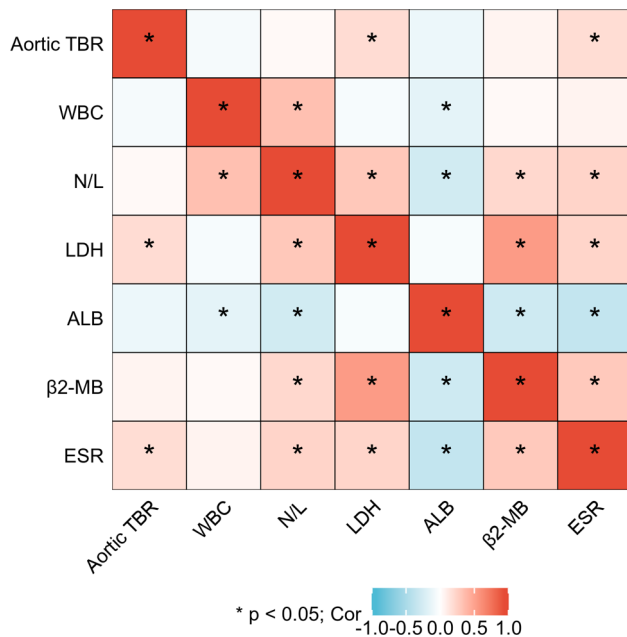


Fig. 3 Heatmap of pre-treatment aortic ¹⁸F-FDG uptake and biomarker correlation analysis in patients with diffuse large B-cell lymphoma

Relationship between pre-treatment aortic ¹⁸F-FDG uptake and tumor metabolic load and biomarkers in patients with diffuse large B-cell lymphoma

Correlation analysis of pre-treatment aortic ¹⁸F-FDG uptake with tumor metabolic load in patients with diffuse large B-cell lymphoma revealed a positive correlation between aortic TBR and TLG ($P=0.016, R=0.19$), and a positive correlation between aortic TBR and MTV ($P=0.032, R=0.17$), as shown in Fig. 2.

Correlation analysis of pre-treatment aortic ¹⁸F-FDG uptake with biomarkers in patients with diffuse large B-cell lymphoma revealed a positive correlation between aortic TBR and LDH and ESR, with a statistically significant difference ($P < 0.05$), as shown in Fig. 3.

Comparison of clinical data, ¹⁸F-FDG PET/CT parameters and efficacy before and after 6 cycles of treatment in patients with diffuse large B-cell lymphoma

After 6 cycles of treatment, clinical data before and after treatment were compared. Of the patients with diffuse large B-cell lymphoma, 123 (76.40%) achieved complete remission, 20 (12.42%) had partial remission, and 18 (11.18%) experienced disease progression. After 6 cycles of treatment, MTV and TLG levels decreased significantly compared with those before treatment, with a statistically significant difference ($P < 0.05$). Additionally, WBC

Table 3 Comparison of clinical data before and after 6 cycles of treatment for diffuse large B-cell lymphoma

	Diffuse large B-cell lymphoma pre-treatment group(N= 161)	Diffuse large B-cell lymphoma post-treatment group (N= 161)	P value
WBC($\times 10^9/L$)	6.25 \pm 2.85	4.59 \pm 2.20	0.001
N/L	3.65 \pm 2.66	3.46 \pm 3.19	0.573
ESR(mm/h)	15.00(9.00, 25.00)	11(5.00, 19.25)	0.019
LDH(ug/mL)	306.27 \pm 222.24	278.7 \pm 127.09	0.172
Alb(g/L)	39.79 \pm 5.70	41.16 \pm 4.92	0.023
β 2-MB(mg/L)	3.08 \pm 1.18	2.96 \pm 0.98	0.348
Therapeutic effect			
Complete remission(n, %)	-	123(76.40)	-
Partial remission(n, %)	-	20(12.42)	-
Progress(n, %)	-	18(11.18)	-
MTV, cm ³	93.31(31.62, 245.88)	0(0, 10.33)	0.001
TLG, g	864.67(246.65, 3113.25)	0(0, 27.25)	0.001

Table 4 Comparison of outcomes of 6 cycles of treatment for different stages of diffuse large B-cell lymphoma

	ANN Arbor Stage I/II (N= 39)	Ann Arbor Stage III/IV (N= 122)	P value
Therapeutic effect			0.62
Complete remission(n, %)	30(76.92)	93(76.23)	
Partial remission(n, %)	6(15.38)	14(11.48)	
Progress(n, %)	3(7.69)	15(12.30)	

count and sedimentation rate decreased significantly compared with pre-treatment levels ($P < 0.05$). Albumin levels increased significantly after 6 cycles of treatment ($P < 0.05$). The levels of neutrophil-to-lymphocyte ratio

(N/L), LDH, and β 2-microglobulin decreased compared to pre-treatment levels, but the differences were not statistically significant ($P > 0.05$). See Table 3.

Evaluation of the effect of 6 cycles of treatment on patients with different stages of diffuse large B-cell lymphoma revealed no statistically significant difference between the complete remission rate, partial remission rate, and progression rate between the two groups ($P > 0.05$). See Table 4.

Analysis of changes in aortic ¹⁸F-FDG uptake after 6 cycles of treatment in patients with diffuse large B-cell lymphoma showed that aortic TBR levels were significantly higher post-treatment compared to pre-treatment ($P < 0.05$). Although aortic calcification scores increased after treatment, the difference was not statistically significant ($P > 0.05$). See Fig. 4.

Comparison of aortic TBR difference among diffuse large B-cell lymphoma 6-cycle treatment groups with different therapeutic effects

Patients with diffuse large B-cell lymphoma were categorized into complete remission, partial remission, and progression groups based on their treatment response after 6 cycles. Comparing the difference in aortic TBR before and after treatment among the three groups showed that the worse the treatment efficacy, the higher the aortic Δ TBR. The progression group had a significantly higher aortic Δ TBR value than the complete remission group ($P < 0.05$). See Fig. 5. Figure 6 shows a lymphoma patient with diffuse uptake in the aortic wall after treatment (red arrow).

A DLBCL case imaged by ¹⁸F-FDG PET/CT examination prior to and after treatment. (A) Sagittal PET images after treatment and (B) before treatment by R-CHOP in a 60-year-old female patient with DLBCL. Red arrows

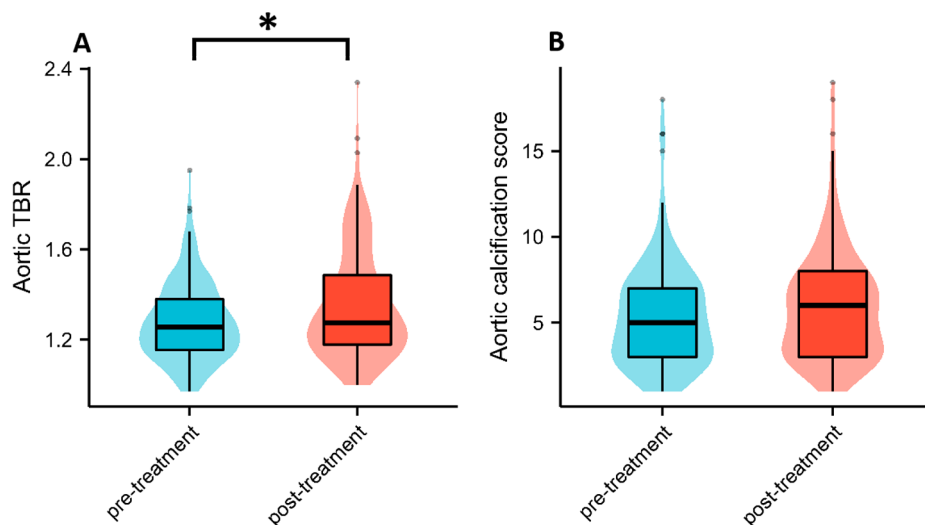


Fig. 4 Comparison of ¹⁸F-FDG PET/CT parameters before and after the 6-cycle treatment group for diffuse large B-cell lymphoma

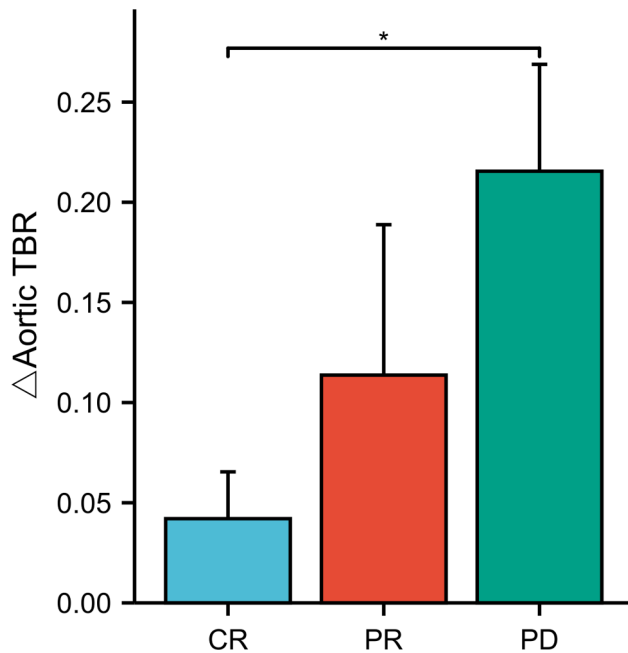


Fig. 5 Comparison of aortic TBR differences between different efficacies in 6-cycle treatment groups for diffuse large B-cell lymphoma

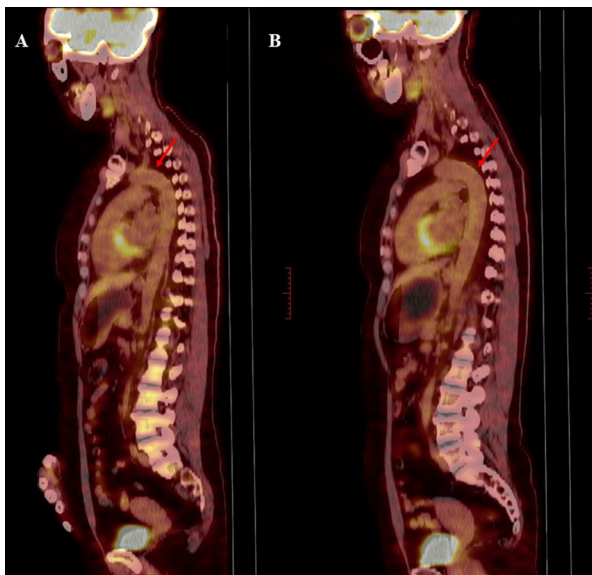


Fig. 6 Enhanced vascular ^{18}F -FDG uptake after treatment compared to before treatment (A: after treatment; B: before treatment)

indicate diffuse increased ^{18}F -FDG uptake on the aortic wall area after R-CHOP treatment. The aortic TBR was 1.24 (the ascending aorta TBR was 1.29, aortic arch TBR was 1.29, descending aorta TBR was 1.12, suprarenal abdominal aorta TBR was 1.29 and infrarenal abdominal aorta was 1.18) after treatment, compared to 1.13 (the ascending aorta TBR was 1.17, aortic arch TBR was 1.11, descending aorta TBR was 1.11, suprarenal abdominal

aorta TBR was 1.17 and infrarenal abdominal aorta was 1.11) before treatment

Discussion

^{18}F -FDG PET/CT is a functional molecular imaging test widely used in oncology and inflammatory diseases to assess arterial inflammation [18]. The selective uptake of metabolically active macrophages within the vessel wall or atherosclerotic plaque is observed by ^{18}F -FDG PET/CT, allowing for quantitative evaluation of vascular inflammation using the TBR of the vessel wall. Previous studies have used ^{18}F -FDG PET/CT to assess aortic inflammation within 72 h of admission and 30 to 45 days after discharge to evaluate changes in vascular inflammation by TBR [19]. Janssen et al. [20] observed changes in immune inflammatory factors due to chronic hyperglycemia in patients with type 1 diabetes and noted increased inflammation in the arterial wall leading to atherosclerosis using ^{18}F -FDG PET/CT. Our group also investigated the effect of COVID-19 on the vascular inflammatory response by using PET/CT to detect ^{18}F -FDG uptake in the systemic arterial wall of patients with diffuse large B-cell lymphoma before and after COVID-19 infection [21]. Similarly, ^{18}F -FDG PET/CT can be used to observe vascular-related complications during the treatment of tumor patients. Villena et al. [22] retrospectively analyzed the predictive value of arterial inflammation for cardiovascular events in 274 patients with primary lung tumors who underwent ^{18}F -FDG PET/CT. Beall et al. [23] used ^{18}F -FDG PET/CT to assess venous inflammation as a predictor of venous thromboembolism in children, adolescents, and young adults within 12 months of lymphoma diagnosis. Therefore, this study focused on observing aortic ^{18}F -FDG uptake before and after applying the R-CHOP regimen in patients with non-Hodgkin's lymphoma.

In this study, various segments of the aorta—including the ascending aorta, aortic arch, descending aorta, suprarenal abdominal aorta, and infrarenal abdominal aorta—were selected to assess the level of ^{18}F -FDG uptake in the arterial wall. It was found that pre-treatment aortic TBR levels were significantly higher in patients with diffuse large B-cell lymphoma compared to control patients. Additionally, patients with stage III/IV diffuse large B-cell lymphoma had significantly higher aortic TBR levels than those with stage I/II disease. Correlation analysis revealed that pre-treatment aortic TBR was positively correlated with TLG and MTV of the lesions observed in PET/CT. Furthermore, aortic TBR was positively correlated with LDH, reflecting the severity of the disease, and ESR, reflecting the level of inflammation. This aligns with the results of previous studies. Tumorigenic mutations may promote local and systemic inflammatory responses [24], stimulating the secretion of pro-inflammatory mediators.

This process allows the differentiation and activation of local immune cells, including neutrophils and monocytes, within the tumor microenvironment [25]. The activation of NF- κ B triggers phagocytosis, engulfing the necrotic residues produced by pro-inflammatory cells and generating a local inflammatory response [26]. When activated monocytes differentiate into macrophages within the vessel wall, they stimulate the secretion of local inflammatory factors, which in turn promotes a vascular inflammatory response [27].

Treatment modalities for non-Hodgkin's lymphoma include chemotherapy, radiotherapy, targeted therapies, and combination therapies. R-CHOP (rituximab, cyclophosphamide, doxorubicin, vincristine, and prednisone) is considered the first-line treatment for diffuse large B-cell lymphoma [28]. In this regimen, various antitumor drugs can cause endothelial cell damage, oxidative stress, and increased cytokine release [29]. Anthracyclines, in particular, increase the levels of endothelial progenitor cells that have lost their ability to repair, leading to impaired endothelial cell repair and exacerbated vascular injury [30]. Several studies have assessed vascular inflammation and injury during tumor radiotherapy and chemotherapy using ^{18}F -FDG PET/CT. Chen et al. [31] evaluated carotid ^{18}F -FDG uptake before and after radiotherapy in 22 patients with head and neck tumors undergoing concurrent radiotherapy. They found that carotid TBR was significantly elevated, and the carotid inflammatory response increased after radiotherapy, correlating with a high risk of future cardiovascular events. They suggested that carotid ^{18}F -FDG uptake may be an early marker of radiotherapy-related vascular injury. In this study, a significant increase in aortic TBR was found in patients with non-Hodgkin's lymphoma after 6 cycles of R-CHOP treatment. This finding contrasts with a study by Lawal et al. [32], which observed no significant change in arterial TBR in 52 patients with Hodgkin's lymphoma who underwent anthracycline-based chemotherapy over 65 weeks of follow-up. The discrepancy may be due to the short-term observation of vascular damage in our study, which measured ^{18}F -FDG uptake in the aorta shortly after 6 consecutive cycles of chemotherapy. It remains to be seen whether these vascular inflammatory responses diminish after chemotherapy cessation or cause sustained vascular damage. Future follow-up should monitor changes in aortic ^{18}F -FDG uptake and the occurrence of vascular events. Interestingly, our study found that changes in aortic TBR before and after R-CHOP treatment varied with treatment effectiveness; the worse the treatment outcome, the greater the difference in aortic TBR. This difference may reflect both the drug-induced vascular damage and the impact of tumor-released inflammatory factors on the blood vessels.

Further research is needed to explore the specific mechanisms involved.

In this study, we also observed changes in aortic calcification before and after treatment using ^{18}F -FDG PET/CT during follow-up. Although the aortic calcification score increased after treatment compared to before treatment, the difference was not statistically significant. This may be due to the shorter treatment cycle and follow-up time. However, several previous studies have highlighted the importance of observing changes in aortic or coronary calcification during oncology treatment follow-up with ^{18}F -FDG PET/CT in predicting cardiovascular events in patients. Mais et al. [33] found that the coronary artery calcium (CAC) score was associated with the risk of clinical events in cancer patients during ^{18}F -FDG PET/CT follow-up, and an increased CAC score was linked to shorter survival times in metastasis-free patients. Gal et al. [34] retrospectively analyzed 15,915 breast cancer patients who received radiotherapy and used follow-up CAC scores to predict the risk of cardiovascular disease. They identified breast cancer patients at increased risk of cardiovascular disease using tools like CT, which are rapid and low-cost. Similarly, observing CAC changes during multiple PET/CT examinations can increase the value of PET/CT as a diagnostic tool. Therefore, monitoring arterial calcification changes is crucial for predicting prognosis and cardiovascular events in tumor patients.

Limitations and prospects

The published European Association of Nuclear Medicine (EANM) position paper on the use of ^{18}F -FDG-PET in atherosclerosis recommends an interval of 2 h between ^{18}F -FDG administration and acquisition [15]. However, currently, there is not enough evidence to apply the same time window for large vessel vasculitis [14]. At this time, EANM recommend an uptake interval of at least 60 min [14]. For arterial imaging with PET, longer delays between ^{18}F -FDG injection and PET imaging than those used for oncology may allow sufficient ^{18}F -FDG accumulation in the arterial wall and to reduce the intensity of ^{18}F -FDG signal in the blood [35]. Our study was a retrospective analysis of clinically indicated imaging and, therefore, the PET/CT scans were performed for clinical indications to assess cancer rather than specifically for vascular assessments.

Although observing ^{18}F -FDG PET/CT during only 6 cycles of treatment suggests the effects of both the tumor and the chemotherapeutic agents on blood vessels, the effects of chemotherapeutic agents on blood vessels and the occurrence of cardiovascular events still require further follow-up. In the future, in addition to further extending the follow-up time, we should also pay more attention to the observation of coronary ^{18}F -FDG uptake changes and calcifications, although noncontract

CT is not very clear for coronary artery imaging, but for lymphoma patients in the process of follow-up oncologic PET/CT, it is very important to strengthen the observation of local coronary artery changes and predict the occurrence of acute coronary events, which is very important to prevent serious complications and improve patient survival.

Conclusion

In this study, in addition to observing lymphoma lesions using PET/CT imaging, changes in ^{18}F -FDG uptake by the aortic wall and changes in aortic calcification were monitored during the ^{18}F -FDG PET/CT follow-up of diffuse large B-cell lymphoma patients undergoing 6 cycles of R-CHOP treatment, before and twice after treatment. It was found that ^{18}F -FDG uptake in the aortic wall before treatment could predict the severity of the disease in lymphoma patients to some extent. The increase in ^{18}F -FDG uptake in the aortic wall after treatment reflected the inflammatory response caused by chemotherapeutic drugs to the blood vessel wall. Additionally, changes in ^{18}F -FDG uptake in the aortic wall before and after treatment also reflected the therapeutic efficacy in lymphoma patients.

Acknowledgements

Thanks to all the peer reviewers and editors for their opinions and suggestions.

Author contributions

Runlong Lin, Jin Wang and Lixiu Cao contributed to the study conception and design. Material preparation, data collection and analysis were performed by Wenli Xie, Jing Yu, Aijuan Tian and Runlong Lin. The first draft of the manuscript was written by Wenli Xie and all authors commented on previous versions of the manuscript. All authors read and approved the final manuscript.

Funding

This work was supported by grants from the Natural Science Foundation of Liaoning Province(2024-BS-184), Basic Scientific Research Program of Education Department of Liaoning Province (No. LJKMZ20221288), Dalian Medical Science Research Program (No.2112011) and "1+X" Research Project of the Second Hospital of Dalian Medical University (2024LJCJYL16).

Data availability

Data is provided within the manuscript or supplementary information files. All datasets and materials used and/or analyzed during the current study are available from the corresponding authors on any reasonable request.

Declarations

Ethical approval

Ethics approval and consent to participate. The study conforms to the ethical guidelines in accordance with the Helsinki Declaration and was approved by the Second Hospital of Dalian Medical University review board and ethical committee (No.2019-049). Written informed consent was obtained from every patient.

Consent for publication

Not applicable.

Clinical trial number

Not applicable.

Competing interests

The authors declare no competing interests.

Author details

¹Department of Cardiovascular Medicine, The Second Hospital of Dalian Medical University, Dalian, People's Republic of China

²Hebei Key Laboratory of Molecular Oncology, Tangshan, People's Republic of China

³Department of Emission Computer Tomography, Tangshan People's Hospital, Tangshan, People's Republic of China

⁴Department of Nuclear Medicine, The Second Hospital of Dalian Medical University, Dalian, People's Republic of China

⁵Department of Vascular Surgery, The Second Hospital of Dalian Medical University, Dalian, People's Republic of China

⁶Department of Nuclear Medicine, The Second Hospital of Dalian Medical University, No.467 Zhongshan Road, Dalian, Liaoning 116023, People's Republic of China

⁷Department of Vascular Surgery, The Second Hospital of Dalian Medical University, No.467 Zhongshan Road, Dalian, Liaoning 116023, People's Republic of China

Received: 21 December 2024 / Accepted: 25 February 2025

Published online: 07 March 2025

References

1. Karlstaedt A, Moslehi J, de Boer RA. Cardio-onco-metabolism: metabolic remodelling in cardiovascular disease and cancer. *Nat Rev Cardiol*. 2022;19(6):414–25.
2. Clayton ZS, Hutton DA, Mahoney SA, Seals DR. Anthracycline chemotherapy-mediated vascular dysfunction as a model of accelerated vascular aging. *Aging Cancer*. 2021;2(1–2):45–69.
3. Herrmann J, Lenihan D, Armenian S, Barac A, Blaes A, Cardinale D, Carver J, Dent S, Ky B, Lyon AR, et al. Defining cardiovascular toxicities of cancer therapies: an international Cardio-Oncology society (IC-OS) consensus statement. *Eur Heart J*. 2022;43(4):280–99.
4. Campia U. Vascular effects of cancer treatments. *Vasc Med*. 2020;25(3):226–34.
5. Patil S, Kata R, Teichner E, Subtirelu R, Ghonim M, Ghonim M, Al-Daoud O, Ismoilov M, Herpin L, Ayubcha C et al. Associations of subclinical microcalcification and inflammation with carotid atheroma development: a dual-tracer PET/CT study. *Eur J Nucl Med Mol Imaging*. 2025.
6. Figueroa AL, Subramanian SS, Cury RC, et al. Distribution of inflammation within carotid atherosclerotic plaques with high-risk morphological features: a comparison between positron emission tomography activity, plaque morphology, and histopathology. *Circ Cardiovasc Imaging*. 2012;5(1):69–77.
7. Kubota R, Yamada S, Kubota K, Ishiwata K, Tamahashi N, Ido T. Intratumoral distribution of fluorine-18-fluorodeoxyglucose in vivo: high accumulation in macrophages and granulation tissues studied by microautoradiography. *J Nucl Med*. 1992;33(11):1972–80.
8. Hecht HS, Cronin P, Blaha MJ, et al. 2016 SCCT/STR guidelines for coronary artery calcium scoring of Noncontrast noncardiac chest CT scans: A report of the society of cardiovascular computed tomography and society of thoracic radiology. *J Thorac Imaging*. 2017;32(5):W54–66.
9. Shen H, Lian Y, Yin J, et al. Cardiovascular risk stratification by automatic coronary artery calcium scoring on pretreatment chest computed tomography in diffuse large B-Cell lymphoma receiving Anthracycline-Based chemotherapy: A multicenter study. *Circ Cardiovasc Imaging*. 2023;16(2):e014829.
10. de Booysson H, Dumont A, Liozon E, et al. Giant-cell arteritis: concordance study between aortic CT angiography and FDG-PET/CT in detection of large-vessel involvement. *Eur J Nucl Med Mol Imaging*. 2017;44(13):2274–9.
11. Boellaard R, Delgado-Bolton R, Oyen WJ, et al. FDG PET/CT: EANM procedure guidelines for tumour imaging: version 2.0. *Eur J Nucl Med Mol Imaging*. 2015;42(2):328–54.
12. Toutouzas K, Skoumas J, Koutagiar I, et al. Vascular inflammation and metabolic activity in hematopoietic organs and liver in Familial combined hyperlipidemia and heterozygous Familial hypercholesterolemia. *J Clin Lipidol*. 2018;12(1):33–43.
13. Brili S, Oikonomou E, Antonopoulos AS, et al. ^{18}F -Fluorodeoxyglucose positron emission tomography/computed tomographic imaging detects aortic wall inflammation in patients with repaired coarctation of aorta. *Circ Cardiovasc Imaging*. 2018;11(1):e007002.

14. Slart R, FDG-PET/CT. (A) imaging in large vessel vasculitis and polymyalgia rheumatica: joint procedural recommendation of the EANM, SNMMI, and the PET interest group (PIG), and endorsed by the ASNC. *Eur J Nucl Med Mol Imaging*. 2018;45(7):1250–69.
15. Bucnerius J, Hyafil F, Verberne HJ, Slart RH, Lindner O, Sciagra R, Agostini D, Übleis C, Gimelli A, Hacker M. Position paper of the cardiovascular committee of the European association of nuclear medicine (EANM) on PET imaging of atherosclerosis. *Eur J Nucl Med Mol Imaging*. 2016;43(4):780–92.
16. Brown ER, Kronmal RA, Bluemke DA, et al. Coronary calcium coverage score: determination, correlates, and predictive accuracy in the Multi-Ethnic study of atherosclerosis. *Radiology*. 2008;247(3):669–75.
17. Rominger A, Saam T, Wolpers S, et al. 18F-FDG PET/CT identifies patients at risk for future vascular events in an otherwise asymptomatic cohort with neoplastic disease. *J Nucl Med*. 2009;50(10):1611–20.
18. Naik HB, Natarajan B, Stansky E, et al. Severity of psoriasis associates with aortic vascular inflammation detected by FDG PET/CT and neutrophil activation in a prospective observational study. *Arterioscler Thromb Vasc Biol*. 2015;35(12):2667–76.
19. Boczar KE, Dwivedi G, Tavoosi A, et al. Vascular inflammation during and after Community-Acquired pneumonia as measured by (18)F-FDG-PET/CT imaging. *JACC Cardiovasc Imaging*. 2023;16(4):562–4.
20. Janssen A, van Heck J, Stienstra R, et al. Arterial wall inflammation assessed by 18F-FDG-PET/CT is higher in individuals with type 1 diabetes and associated with Circulating inflammatory proteins. *Cardiovasc Res*. 2023;119(10):1942–51.
21. Lin R, Yu J, Tian A, et al. Time-Related vascular inflammatory response to COVID-19 assessed by (18)F-FDG PET/CT in Follow-Up tumor patients. *J Inflamm Res*. 2023;16:3109–17.
22. Villena García AC, Cardo AG, Hidalgo CM, et al. 18FDG PET/CT & arterial inflammation: predicting cardiovascular events in lung cancer. *QJM*. 2019;112(6):401–7.
23. Beall M, Deep K, Tram NK, et al. Prognostic value of Fluorine-18-Fluorodeoxyglucose positron emission tomography/computed tomography imaging for predicting venous thromboembolism in children with lymphoma. *Circ Cardiovasc Imaging*. 2023;16(4):e014992.
24. Mantovani A, Allavena P, Sica A, Balkwill F. Cancer-related inflammation. *Nature*. 2008;454(7203):436–44.
25. Nie M, Yang L, Bi X, et al. Neutrophil extracellular traps induced by IL8 promote diffuse large B-cell lymphoma progression via the TLR9 signaling. *Clin Cancer Res*. 2019;25(6):1867–79.
26. Scott DW, Gascoyne RD. The tumour microenvironment in B cell lymphomas. *Nat Rev Cancer*. 2014;14(8):517–34.
27. Diakos CI, Charles KA, McMillan DC, Clarke SJ. Cancer-related inflammation and treatment effectiveness. *Lancet Oncol*. 2014;15(11):e493–503.
28. Ollila TA, Olszewski AJ, Extranodal Diffuse Large B, Cell Lymphoma. Molecular features, prognosis, and risk of central nervous system recurrence. *Curr Treat Options Oncol*. 2018;19(8):38.
29. van Nimwegen FA, Schaapveld M, Janus CP, et al. Cardiovascular disease after hodgkin lymphoma treatment: 40-year disease risk. *JAMA Intern Med*. 2015;175(6):1007–17.
30. Wiessman M, Leshem D, Yeshurun M, et al. Dysfunctional endothelial progenitor cells in patients with Hodgkin's lymphoma in complete remission. *Cancer Med*. 2019;8(1):305–10.
31. Chen X, Zheng Y, Tatsuoka C, et al. Chemoradiotherapy-related carotid artery inflammation in head and neck cancer patients quantified by [(18)F]FDG PET/CT. *Oral Oncol*. 2019;93:101–6.
32. Lawal IO, Orunmuyi AT, Popoola GO, et al. FDG PET/CT for evaluating systemic arterial inflammation induced by anthracycline-based chemotherapy of hodgkin lymphoma: A retrospective cohort study. *Med (Baltim)*. 2020;99(48):e23259.
33. Mais HE, Kay R, Almubarak H, et al. Prognostic importance of coincidental coronary artery calcification on FDG-PET/CT oncology studies. *Int J Cardiovasc Imaging*. 2021;37(4):1479–88.
34. Gal R, van Velzen S, Hooning MJ, et al. Identification of risk of cardiovascular disease by automatic quantification of coronary artery calcifications on radiotherapy planning CT scans in patients with breast Cancer. *JAMA Oncol*. 2021;7(7):1024–32.
35. Lawal IO, Mokoala KG, Popoola GO, Lengana T, Ankrah AO, Stoltz AC, Sath-ekke MM. Impact of optimized PET imaging conditions on (18)F-FDG uptake quantification in patients with apparently normal aortas. *J Nucl Cardiol*. 2021;28(4):1349–59.

Publisher's note

Springer Nature remains neutral with regard to jurisdictional claims in published maps and institutional affiliations.